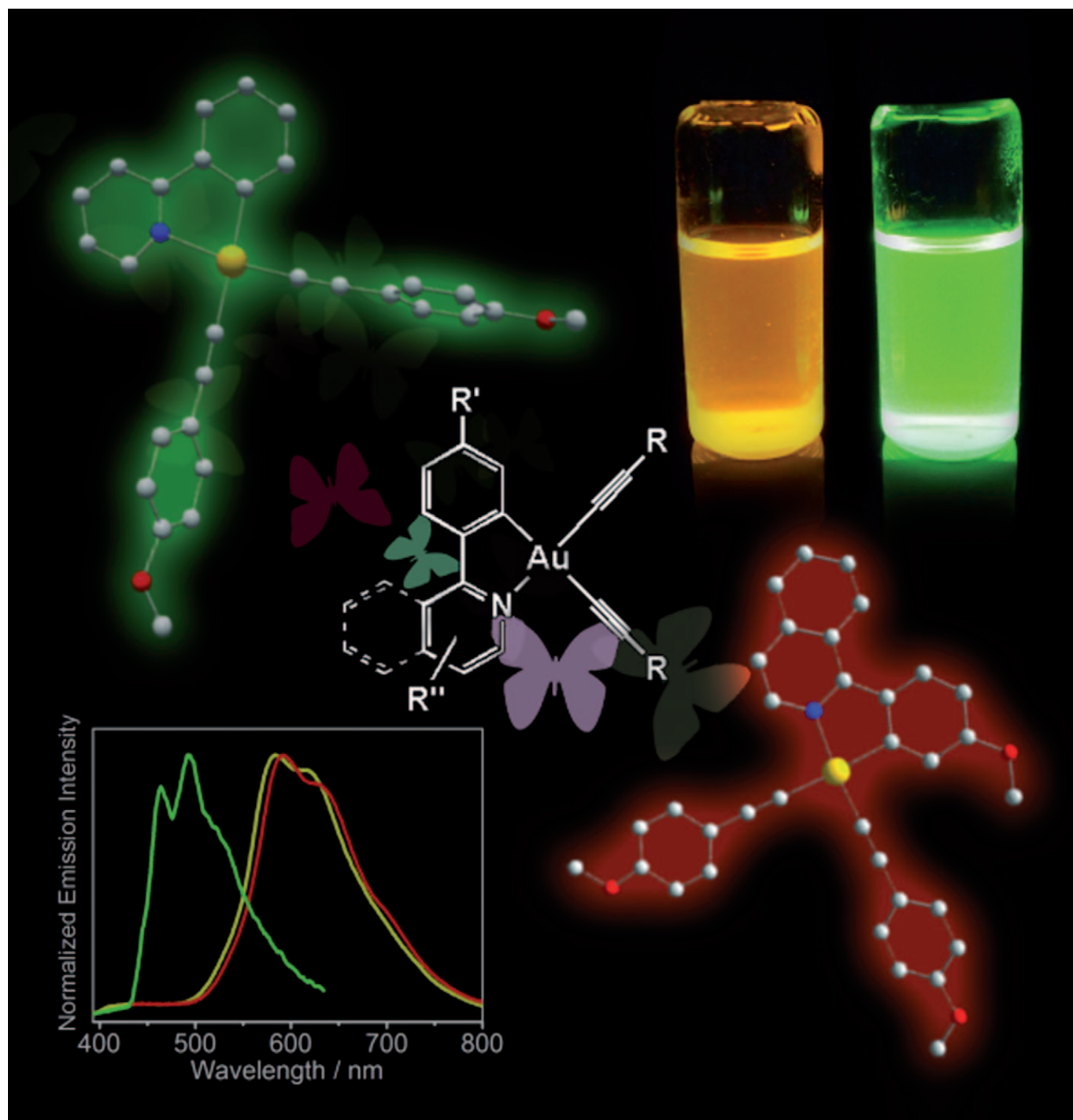


Luminescent Cyclometalated Dialkynylgold(III) Complexes of 2-Phenylpyridine-Type Derivatives with Readily Tunable Emission Properties

Vonika Ka-Man Au, Keith Man-Chung Wong, Nianyong Zhu, and Vivian Wing-Wah Yam^{*[a]}



Abstract: A novel class of luminescent dialkynylgold(III) complexes containing various phenylpyridine and phenylisoquinoline-type bidentate ligands has been successfully synthesized and characterized. The structures of some of them have also been determined by X-ray crystallography. Electrochemical studies demonstrate the presence of a ligand-centered reduction originating from the cyclometalating C[^]N ligand, whereas the first oxidation wave is associated with an alkynyl ligand-centered oxidation. The electronic absorption and photoluminescence properties

of the complexes have also been investigated. In dichloromethane solution at room temperature, the low-energy absorption bands are assigned as the metal-perturbed π - π^* intraligand (IL) transition of the cyclometalating C[^]N ligand, with mixing of charge-transfer character from the aryl ring to the pyridine or isoquinoline moieties of the cyclometalating C[^]N ligand. The low-

energy emission bands of the complexes in fluid solution at room temperature are ascribed to originate from the metal-perturbed π - π^* IL transition of the cyclometalating C[^]N ligand. For complex **4** that contains an electron-rich amino substituent on the alkynyl ligand, a structureless emission band, instead of one with vibronic structures as in the other complexes, was observed, which was assigned as being derived from an excited state of a $[\pi(\text{C}\equiv\text{C}_6\text{H}_4\text{NH}_2)\rightarrow\pi^*(\text{C}^{\wedge}\text{N})]$ ligand-to-ligand charge-transfer (LLCT) transition.

Keywords: acetylides • cyclometalation • excited states • gold • luminescence

Introduction

Over the past decade, there has been an enormous growth in the research and development of new luminophores for applications in efficient organic light-emitting devices (OLEDs). In particular, much attention has been drawn towards the use of heavy-metal complexes, in which strong spin-orbit coupling occurs to allow intersystem crossing (ISC) between singlet and triplet states, resulting in much higher quantum yield of emission from the triplet state, thereby improving the internal quantum efficiency of OLEDs to 100%.^[1] Baldo et al. reported the first use of the [Ir(ppy)₃] (ppy = 2-phenylpyridine) phosphorescent emitting material as a dopant in a 4,4'-N,N'-dicarbazolebiphenyl (CBP) host to give high quantum efficiency OLEDs.^[1] In light of the rich photoluminescence properties of [Ir(ppy)₃], there has also been a growing interest in the incorporation of 2-phenylpyridine derivatives and other cyclometalating C[^]N ligands into iridium(III) centers to prepare triplet emitters for OLED applications.^[2] An important advantage of the use of cyclometalating ligands is that by varying the substituents, the emission color of the resulting metal complexes can be readily tuned over the visible region. Despite this, the use of ppy-type phosphors containing alternative metal centers remains relatively less extensively explored and rather underdeveloped, with only some reports on ppy derivatives of platinum(II)^[3] and ruthenium(II).^[4]

In contrast to the isoelectronic platinum(II) compounds that are known to show rich luminescence properties,^[5] very

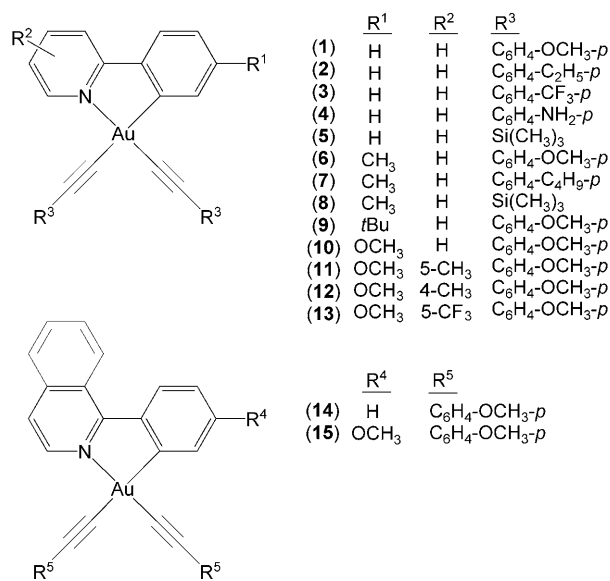
few examples of luminescent gold(III) complexes have been reported,^[6] which probably stems from the presence of low-energy d-d ligand field (LF) states and the electrophilicity observed for the gold(III) metal center.^[6] One way to enhance the luminescence of gold(III) complexes is by introduction of strong σ -donating ligands, which was first demonstrated by our group on stable gold(III) aryl compounds that were found to display interesting photoluminescence properties even at room temperature.^[7] This concept has been further extended and demonstrated in gold(III) complexes containing the tridentate bis-cyclometalating diarylpyridine (C[^]N[^]C)-type ligands with alkynyls and *N*-heterocyclic cyclic carbenes as the σ -donating ancillary ligands, all of which exhibit rich luminescence behaviors at both room and low temperatures in various media.^[8,9] Although gold(III) complexes containing various bidentate cyclometalating C[^]N ligands have been reported, their photophysical studies have rarely been investigated.^[10,11] It is envisaged that the use of cyclometalating C[^]N-type ligands in combination with alkynyl ligands would result in interesting organogold(III) complexes with rich luminescence behaviors. In addition, by the judicious selection of the bidentate cyclometalating ligand, the emission color of the gold(III) complexes can be readily tuned. Herein we report the synthesis, characterization, electrochemical, and photophysical studies of a versatile class of luminescent dialkynylgold(III) complexes with various cyclometalating and alkynyl ligands, [Au(C[^]N)(C \equiv CR)₂]. To the best of our knowledge, this is the first report on luminescent gold(III) complexes containing bidentate C[^]N ligands that exhibit luminescence at room temperature.

Results and Discussion

Synthesis and characterization: All dichlorogold(III) precursor complexes, [Au(C[^]N)Cl₂]^[12] were prepared according to a literature procedure by using various cyclometalating C[^]N

[a] V. K.-M. Au, Dr. K. M.-C. Wong, Dr. N. Zhu, Prof. Dr. V. W.-W. Yam
Institute of Molecular Functional Materials
and Department of Chemistry
The University of Hong Kong
Pokfulam Road, Hong Kong (P.R. China)
Areas of Excellence Scheme
University Grants Committee (Hong Kong)
Fax: (+0852)2857-1586
E-mail: wwyam@hku.hk

ligands that are either commercially available or synthesized through Suzuki coupling reactions.^[13] The dialkynylgold(III) complexes **1–15** were prepared according to the reaction of



the respective dichlorogold(III) precursor compounds with the various alkynyllithium reagents, which were prepared in situ from *n*-butyllithium and the respective alkynes in tetrahydrofuran under a nitrogen atmosphere at -78°C . All the

complexes were found to be air stable, thermally stable, and could be stored over extended periods of up to several months in the dark. Compared with the dichlorogold(III) precursor complexes, the dialkynylgold(III) complexes were found to be much more soluble in common organic solvents like dichloromethane. The identities of all the complexes, namely **1–15**, have been confirmed by ^1H NMR spectroscopy, FAB mass spectrometry, and satisfactory elemental analyses. The crystal structures of **1**, **6**, **11**, **12**, and **15** have also been determined by X-ray crystallography. In general, their IR spectra exhibited two $\tilde{\nu}(\text{C}\equiv\text{C})$ absorptions at $2075\text{--}2191\text{ cm}^{-1}$, which is in accordance with the configuration of two alkynyl ligands in the *trans* position to N and C atoms on the cyclometalating ligands. Similarly, the NMR signals of the phenyl protons on the two alkynyl ligands in their ^1H NMR spectra were at different chemical shifts because these two alkynyl ligands are not chemically equivalent.

X-ray crystal structures: Single crystals of **1**, **6**, **11**, **12**, and **15** were obtained by layering of *n*-hexane onto a concentrated dichloromethane solution of the complexes, and their structures were solved by X-ray crystallography. Crystal-structure determination data are summarized in Table 1. The selected bond distances and bond angles as well as selected intermolecular parameters are tabulated in Table 2. The perspective views of the crystal structures of **1**, **6**, **11**, **12**, and **15** are depicted in Figure 1. In each case, the gold(III) metal center coordinates to the bidentate cyclometalating C[∧]N ligand with the remaining two sites each occupied

Table 1. Crystal and structure determination data of **1**, **6**, **11**, **12**, and **15**.

Complex	1	6	11 - CH_2Cl_2	12 - CH_2Cl_2	15 - CH_2Cl_2
formula	$\text{C}_{29}\text{H}_{22}\text{AuNO}_2$	$\text{C}_{30}\text{H}_{24}\text{AuNO}_2$	$\text{C}_{32}\text{H}_{28}\text{AuCl}_2\text{NO}_3$	$\text{C}_{32}\text{H}_{28}\text{AuCl}_2\text{NO}_3$	$\text{C}_{35}\text{H}_{28}\text{AuCl}_2\text{NO}_3$
M_r	613.46	627.47	742.42	742.42	778.45
T [K]	301(2)	301(2)	301(2)	301(2)	301(2)
λ [Å]	0.71073	0.71073	0.71073	0.71073	0.71073
crystal system	monoclinic	monoclinic	monoclinic	monoclinic	monoclinic
space group	$P2_1/c$	$P2_1/n$	$P2_1/c$	$P2_1/c$	$P2_1/c$
a [Å]	10.5506(12)	13.9463(6)	15.199(1)	11.853(1)	12.0236(7)
b [Å]	19.151(2)	12.9040(6)	8.5757(8)	11.584(1)	11.5276(6)
c [Å]	11.839(1)	14.0662(6)	23.146(2)	21.840(3)	22.288(1)
α [°]	90	90	90	90	90
β [°]	102.384(2)	103.273(1)	104.89(1)	94.04(2)	94.77(1)
γ [°]	90	90	90	90	90
V [cm ³]	2336.5(5)	2463.78(19)	2915.5(4)	2991.2(6)	3078.5(3)
Z [Å ³]	4	4	4	4	4
ρ_{calcd} [g cm ⁻³]	1.744	1.692	1.691	1.649	1.680
crystal size [mm ³]	0.24 × 0.23 × 0.19	0.3 × 0.25 × 0.2	0.4 × 0.16 × 0.05	0.27 × 0.25 × 0.13	0.46 × 0.42 × 0.3
index ranges	$-14 \leq h \leq 12$, $-25 \leq k \leq 25$, $-15 \leq l \leq 13$	$-16 \leq h \leq 18$, $-16 \leq k \leq 15$, $-17 \leq l \leq 18$	$-18 \leq h \leq 18$, $-10 \leq k \leq 10$, $-28 \leq l \leq 26$	$-10 \leq h \leq 14$, $-14 \leq k \leq 14$, $-26 \leq l \leq 25$	$-12 \leq h \leq 14$, $-14 \leq k \leq 14$, $-27 \leq l \leq 24$
reflections collected/unique	16230/5693	14241/5598	16398/5504	17090/5673	17295/5815
GOF on F^2	1.019	1.024	1.044	1.011	1.042
final R indices	$R_1 = 0.0417$, $wR_2 = 0.1004$	$R_1 = 0.0224$, $wR_2 = 0.0520$	$R_1 = 0.0263$, $wR_2 = 0.0651$	$R_1 = 0.0267$, $wR_2 = 0.0589$	$R_1 = 0.0211$, $wR_2 = 0.0466$
largest diff peak and hole [e Å ⁻³]	2.192 and -1.195	1.431 and -0.780	1.164 and -0.743	0.699 and -0.336	0.371 and -0.743

Table 2. Selected bond lengths [\AA] and angles [$^\circ$] for **1**, **6**, **11**, **12**, and **15** with estimated standard deviations (esds) given in parentheses.

1		6		11-CH₂Cl₂		12-CH₂Cl₂		15-CH₂Cl₂	
Au1–N1	2.12(3)	Au1–N1	2.074(3)	Au1–N1	2.067(3)	Au1–N1	2.065(3)	Au1–N1	2.063(2)
Au1–C1	1.95(3)	Au1–C1	2.031(3)	Au1–C19	2.041(4)	Au1–C7	2.038(4)	Au1–C1	2.034(3)
Au1–C21	2.028(7)	Au1–C13	2.037(4)	Au1–C1	2.052(5)	Au1–C23	2.028(5)	Au1–C17	2.034(3)
Au1–C12	1.973(8)	Au1–C22	1.958(4)	Au1–C10	1.957(4)	Au1–C14	1.948(5)	Au1–C26	1.960(3)
C21–C22	1.191(9)	C13–C14	1.194(5)	C1–C2	1.184(6)	C23–C24	1.201(6)	C17–C18	1.199(4)
C12–C13	1.193(10)	C22–C23	1.193(5)	C10–C11	1.194(6)	C14–C15	1.208(6)	C26–C27	1.193(4)
N1–Au1–C1	82.1(11)	N1–Au1–C1	81.17(13)	N1–Au1–C19	81.0(16)	N1–Au1–C7	81.2(15)	N1–Au1–C1	80.6(11)
N1–Au1–C21	96.1(8)	N1–Au1–C13	94.68(14)	N1–Au1–C1	93.8(15)	N1–Au1–C23	96.1(16)	N1–Au1–C17	96.3(11)
N1–Au1–C12	172.9(8)	N1–Au1–C22	173.55(13)	N1–Au1–C10	173.1(15)	N1–Au1–C14	174.2(15)	N1–Au1–C26	173.9(11)
C1–Au1–C12	90.8(9)	C1–Au1–C22	92.58(14)	C19–Au1–C10	92.6(17)	C7–Au1–C14	93.1(15)	C1–Au1–C26	93.2(12)
C1–Au1–C21	177.2(8)	C1–Au1–C13	175.84(14)	C19–Au1–C1	174.8(14)	C7–Au1–C23	177.2(16)	C1–Au1–C17	96.3(11)
C21–Au1–C12	91.0(3)	C13–Au1–C22	91.57(15)	C1–Au1–C10	92.6(17)	C23–Au1–C14	89.6(17)	C17–Au1–C26	89.8(2)
Au1–C21–C22	169.5(6)	Au1–C13–C14	176.6(4)	Au1–C1–C2	169.8(4)	Au1–C23–C24	177.2(4)	Au1–C17–C18	178.0(3)
Au1–C12–C13	176.9(7)	Au1–C22–C23	177.0(3)	Au1–C10–C11	176.8(4)	Au1–C14–C15	178.5(4)	Au1–C26–C27	175.8(3)
C21–C22–C23	176.1(8)	C13–C14–C15	178.2(4)	C1–C2–C3	174.0(4)	C23–C24–C25	177.8(5)	C17–C18–C19	177.5(3)
C12–C13–C14	178.0(8)	C22–C23–C24	177.4(4)	C10–C11–C12	176.7(5)	C14–C15–C16	177.9(5)	C26–C27–C28	178.2(4)

by an alkynyl ligand to give a distorted square-planar geometry, characteristic of d^8 metal complexes. The C–Au–N angles of 80.6 – 82.1° about the gold(III) metal center are found to deviate from the ideal 90° owing to the restricted bite angle of the bidentate $C^{\wedge}N$ ligands. This is accompanied by a concomitant opening of the N–Au–C(alkynyl) (93.8 – 96.3°) and C(alkynyl)–Au–C(alkynyl) (89.6 – 92.6°) bond angles. The same constraints associated with the chelating ligand can also be observed in the dichlorogold(III) precursor^[14a] and related organogold(III) complexes containing $C^{\wedge}N$ ligands.^[14–17] The $[\text{Au}(C^{\wedge}N)]$ motif is essentially coplanar, and the Au–C (2.031 – 2.046 \AA) and Au–N (2.063 – 2.074 \AA) bond lengths are similar to those found in other related complexes.^[14–17] The Au–C and Au–N bond lengths in **1** deviate from the above ranges of values owing to disorder in the C and N atoms of the ppy moiety. The Au–C \equiv C angles range from 169.5 to 178.5° , establishing a slightly distorted linear arrangement, with the Au–C (1.948 – 2.052 \AA) and C \equiv C bond lengths (1.184 – 1.208 \AA) similar to those found in the related bis-cyclometalated alkynylgold(III) system.^[8]

Because the shortest Au \cdots Au distances (5.037 – 7.521 \AA) between adjacent molecules are found to be longer than the sum of van der Waals radii for two gold(III) centers, no significant Au \cdots Au interactions occur in the crystal lattices of the complexes. Moreover, as there is only slight overlap between adjacent $[\text{Au}(C^{\wedge}N)]$ moieties in the complexes, π – π stacking interactions are very weak to negligible in the complexes. The complex molecules are packed in a variety of manners, as depicted in the crystal packing diagrams in Figure 2.

Electrochemistry: The cyclic voltammograms of **1**–**15** in dichloromethane ($n\text{Bu}_4\text{NPF}_6$, TBAH; 0.1 mol dm^{-3}) generally show one quasi-reversible reduction couple at -1.47 to -1.64 V (vs. standard calomel electrode, SCE) and irreversible oxidation waves in the ranges of $+0.87$ to $+1.68 \text{ V}$ (vs. SCE). The electrochemical data are summarized in Table 3. Similar reduction potentials were observed in complexes **1**–

5 and in **6**–**8** consisting of the same $C^{\wedge}N$ ligand. The reduction process is assigned as the ligand-centered reduction of the $C^{\wedge}N$ ligand. The occurrence of this reduction at a more negative potential in **6**–**12** than **1**–**5** is also in line with this assignment because the electron-donating methyl, *tert*-butyl, and methoxy substituents on the $C^{\wedge}N$ ligand would destabilize the π^* orbital and reduce its ease of reduction to give more negative potentials. Conversely, a less negative potential was observed for the reduction couple in **13** owing to the presence of a strongly electron-withdrawing trifluoromethyl group, which would stabilize the π^* orbital, rendering it easier to be reduced. Likewise, an increase in the extent of π -conjugation upon a change from pyridine to the isoquinoline moiety on the $C^{\wedge}N$ ligand would result in a lower-lying π^* orbital, with the ligand-centered reduction potentials of **14** and **15** being less negative than the corresponding ppy analogues **1** and **10**, respectively. Consequently, **14** and **15** both exhibit the least negative reduction potentials among all the complexes studied.

On the other hand, the potentials for the first oxidation were found to be quite sensitive to the nature of the alkynyl ligand. In view of the electron-deficient and redox-inactive nature of the gold(III) metal center, the oxidation wave was assigned as the alkynyl ligand-centered oxidation, as in the related alkynylgold(III) complexes with tridentate bis-cyclometalating ligands.^[8] In general, complexes containing the same alkynyl groups are found to show similar potentials. Complex **4**, which contains the electron-rich aminophenyl alkynyl ligands, exhibited the least positive potential of $+0.87 \text{ V}$ (vs. SCE). No anodic waves could be observed in complexes **5** and **8**, probably due to the lack of the phenyl ring in the ethynyltrimethylsilane ligands. No correlation was found for the second oxidation wave, and the occurrence of this wave is probably due to decompositions that have occurred after the first oxidation process, based on the fact that strong anodic signals that are typical of electrode adsorption were observed upon the reduction scan immediately after the first oxidation.

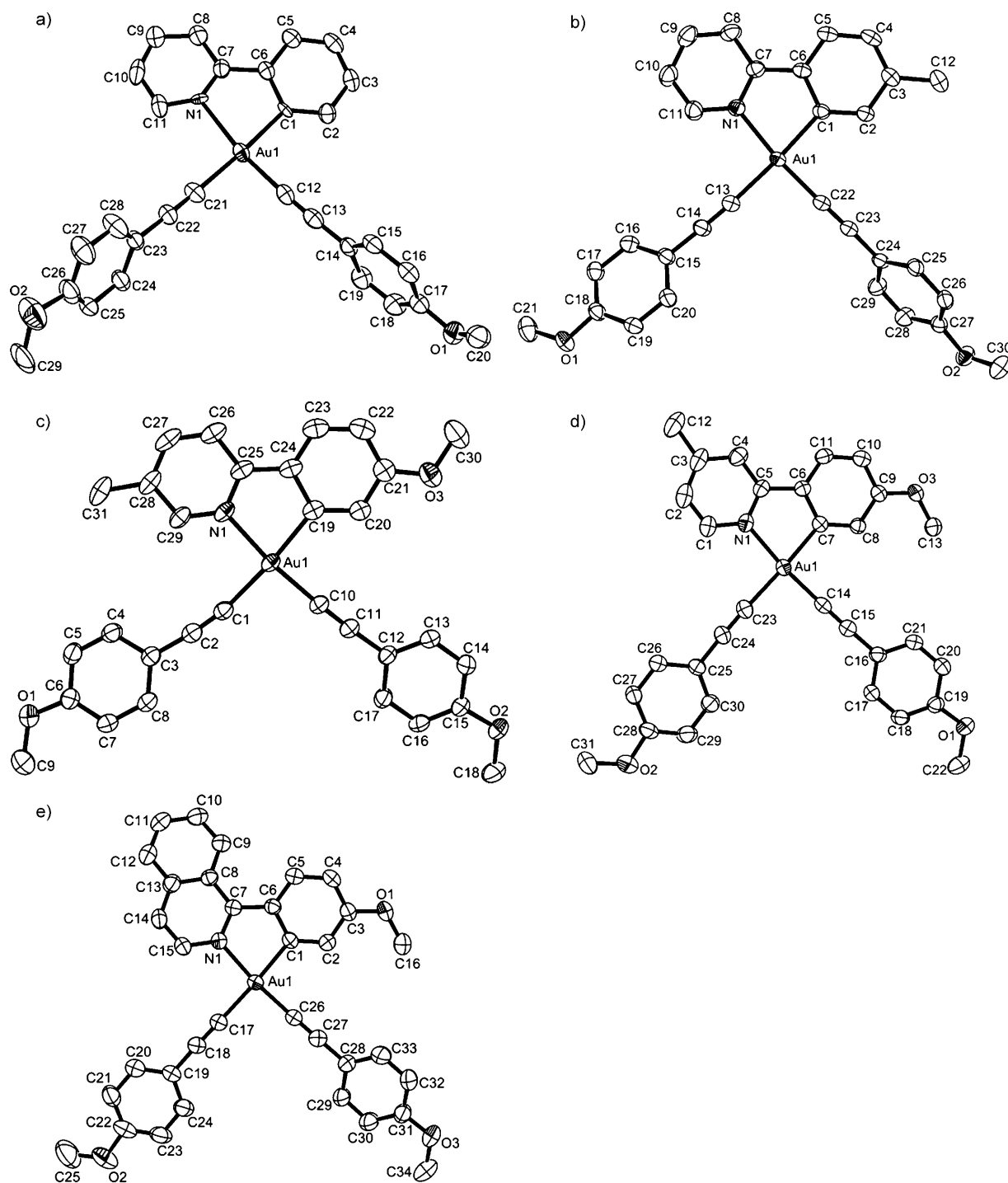


Figure 1. Perspective drawings of complexes a) **1**, b) **6**, c) **11**, d) **12**, and e) **15** with an atomic numbering scheme. Hydrogen atoms and solvent molecules are omitted for clarity. Thermal ellipsoids are drawn at the 30% probability level.

UV/Vis absorption spectroscopy: The UV/Vis absorption spectra of complexes **1–13** in dichloromethane at 298 K exhibit intense absorption bands or shoulders in the 300–370 nm region, whereas complexes **14** and **15**, with the more conjugated phenylisoquinoline-type ligand, show intense absorption bands at approximately 360–416 nm. All the absorption bands show extinction coefficients (ϵ) in the order

of $10^4 \text{ dm}^3 \text{ mol}^{-1} \text{ cm}^{-1}$, with the exception of complexes **5** and **8** that show slightly smaller ϵ values of $7.1\text{--}9.0 \times 10^3 \text{ dm}^3 \text{ mol}^{-1} \text{ cm}^{-1}$ due to the absence of the phenyl ring in the ethynyltrimethylsilane ligands. These results were found to resemble those of the dichlorogold(III) precursors and related complexes reported in the literature.^[10,11] A detailed study has previously been conducted by Eisenberg and co-

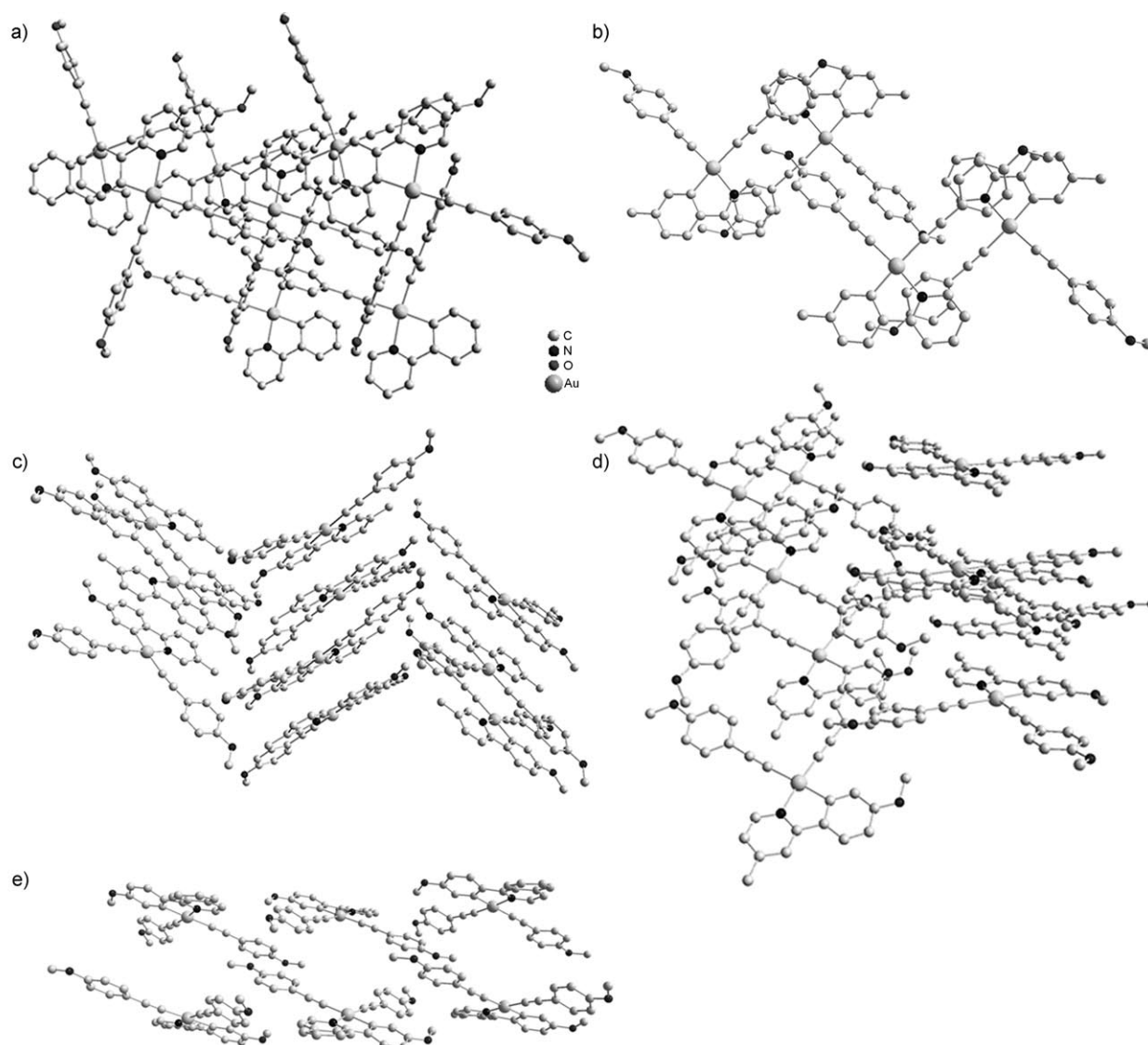


Figure 2. Crystal packing diagrams of complexes a) **1**, b) **6**, c) **11**, d) **12**, and e) **15**.

Table 3. Electrochemical data for **1–15**.^[a]

Complex	Oxidation $E_{pa}^{[b]}$ vs. SCE [V]	Reduction $E_{1/2}^{[c]}$ vs. SCE [V]
1	+1.19, +1.53	-1.51
2	+1.43	-1.51
3	+1.61	-1.47
4	+0.87, +1.10	-1.52
5	_[d]	-1.54
6	+1.26, +1.68	-1.55
7	+1.32, +1.46	-1.52
8	_[d]	-1.57
9	+0.96, +1.50	-1.53
10	+1.11, +1.32	-1.56
11	+1.24, +1.54	-1.60
12	+1.14, +1.37	-1.64
13	+1.29, +1.49	-1.33
14	+1.09, +1.30	-1.26
15	+1.04, +1.24	-1.37

[a] In dichloromethane solution with TBAH (0.1 M) as the supporting electrolyte at room temperature; scan rate 100 mV s⁻¹. [b] E_{pa} refers to the anodic peak potential for the irreversible oxidation waves. [c] $E_{1/2} = (E_{pa} + E_{pc})/2$; E_{pa} and E_{pc} are peak anodic and peak cathodic potentials, respectively. [d] No observable oxidation waves.

workers on the UV/Vis absorption behaviors of the dichlorogold(III) precursor, [Au(ppp)Cl₂], as well as the free ppy ligand.^[10] The dichlorogold(III) complex showed moderately intense absorption bands at 224, 292, and 334 nm, whereas the free ligand peaked at 234 and 290 nm. Because there was insignificant shift in the electronic absorption bands upon complexation, the high-energy bands of the dichlorogold(III) precursor were assigned as intraligand $\pi-\pi^*$ transitions of the ppy ligand. The photophysical data of **1–15** are summarized in Table 4, and the corresponding electronic absorption spectra of **1**, **2**, **4**, **10**, and **13–15** are depicted in Figure 3. Comparison of the UV/Vis absorption behaviors of complexes **1–5** and **6–8** reveals that the high-energy absorption is rather insensitive to the nature of the alkyne ligand. On the other hand, variation of the cyclometalating C[^]N ligands would cause a change in the absorption energies. With reference to such sensitivity to the nature of the cyclometalating C[^]N ligands, together with previous reports on the dichlorogold(III) precursors and the related gold(III) ppy^[10,11] and alkynegold(III) complexes,^[8] the electronic ab-

Table 4. Photophysical data for **1–15**.

Complex	Absorption ^[a] λ_{\max} [nm] (ϵ_{\max} [dm ³ mol ⁻¹ cm ⁻¹])	Medium (<i>T</i> [K])	Emission λ_{\max} [nm] (τ_0 [μs])	Φ_{em} ^[b]
1	300 (16115), 326 (17365)	CH ₂ Cl ₂ (298) ^[c] glass (77) ^[c,d]	464, 492, 524 sh (<0.05) 459, 491, 525, 568 sh (402)	1.7×10^{-2}
2	302 (14370), 320 (16905)	CH ₂ Cl ₂ (298) ^[c] glass (77) ^[c,d]	462, 493, 524 sh (3.4) 457, 491, 524, 565 sh (310)	2.5×10^{-2}
3	318 sh (14455), 330 sh (9685), 346 (5665)	CH ₂ Cl ₂ (298) ^[c] glass (77) ^[c,d]	464, 493, 522 sh (8.0) 458, 492, 521 (381)	1.6×10^{-2}
4	316 sh (24520), 332 sh (19260), 360 sh (9245)	CH ₂ Cl ₂ (298) glass (77) ^[c,d]	441, 613 (<0.05) 455, 490, 518 (197)	2.2×10^{-2}
5	320 (7800), 330 sh (7290), 340 sh (5750)	CH ₂ Cl ₂ (298) ^[c] glass (77) ^[c,d]	462, 493, 523 sh (9.6) 458, 483, 492, 519 (461)	7.1×10^{-2}
6	300 (14180), 330 (16175)	CH ₂ Cl ₂ (298) ^[c] glass (77) ^[c,d]	473, 503, 540 sh (<0.05) 465, 498, 530 (424)	1.8×10^{-2}
7	324 (20575), 354 (7355)	CH ₂ Cl ₂ (298) ^[c] glass (77) ^[c,d]	472, 502, 534 sh (10.3) 464, 499, 526 (433)	1.3×10^{-2}
8	320 sh (7065), 340 (8990), 352 (7485)	CH ₂ Cl ₂ (298) ^[c] glass (77) ^[c,d]	472, 503, 535 sh (12.4) 464, 499, 528 (615)	0.103
9	302 (17630), 330 (21650)	CH ₂ Cl ₂ (298) ^[c] glass (77) ^[c,d]	470, 500, 532 sh (<0.05) 462, 498, 527, 563 sh (433)	2.9×10^{-2}
10	330 (15820), 366 sh (9235), 374 sh (7105)	CH ₂ Cl ₂ (298) ^[c] glass (77) ^[c,d]	487, 514, 553 sh (14.6) 475, 507, 540 (519)	4.6×10^{-2}
11	330 sh (16265), 370 sh (8475)	CH ₂ Cl ₂ (298) ^[c] glass (77) ^[c,d]	491, 520, 556 sh (<0.05) 480, 503, 515, 540 sh (559)	4.5×10^{-2}
12	326 sh (15530), 364 sh (7375)	CH ₂ Cl ₂ (298) ^[c] glass (77) ^[c,d]	479, 507, 549 sh (10.2) 490, 524, 469 sh (463)	2.5×10^{-2}
13	318 (14960), 358 (18175)	CH ₂ Cl ₂ (298) ^[c] glass (77) ^[c,d]	499, 523, 569 sh (6.4) 487, 519, 555 sh (541)	9.9×10^{-2}
14	362 (13565), 398 sh (6665)	CH ₂ Cl ₂ (298) ^[c] glass (77) ^[c,d]	582, 621 (19.4) 573, 619, 673 sh (46.1)	4.5×10^{-2}
15	322 sh (28495), 360 sh (23814), 400 (27910), 416 sh (22930)	CH ₂ Cl ₂ (298) ^[c] glass (77) ^[c,d]	592, 632, 697 sh (30.9) 585, 630, 690 sh (167)	6.0×10^{-2}

[a] In dichloromethane at 298 K. [b] The luminescence quantum yield, measured at room temperature by using quinine sulfate as a standard. [c] Vibronic-structured emission band. [d] In EtOH/MeOH/CH₂Cl₂ (40:10:1 v/v).

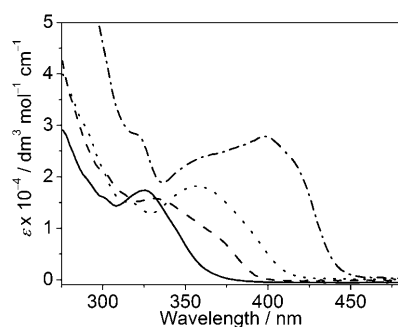


Figure 3. Electronic absorption spectra of **1** (—), **10** (----), **13** (.....), and **15** (-.-.-) in CH₂Cl₂ at room temperature.

sorption band of these dialkynylgold(III) complexes is suggested to be assigned as a metal-perturbed π - π^* intraligand (IL) transition of the C[^]N ligand, with charge-transfer character from the aryl ring to the pyridyl or isoquinoline moiety, probably mixed with some alkynyl-to-cyclometalating ligand LLCT character, given the non-reducing nature of the gold(III) metal center, which eliminates the possibility of a metal-to-ligand charge-transfer (MLCT) transition. Attachment of electron-donating methyl, *tert*-butyl, and the strongly electron-donating methoxy groups on the phenyl

ring in complexes **6–13** has generally resulted in red shifts in the electronic absorption compared with complexes **1–5** that contain the unsubstituted ppy ligand. This is in accordance with the assignment of a metal-perturbed π - π^* (C[^]N) intraligand (IL) transition because the electron-donating groups on the phenyl rings would narrow the HOMO–LUMO energy gap in view of the fact that the energy level of the HOMO π orbital is raised to a larger extent than that of the LUMO π^* orbital. In addition, a pronounced shift to lower absorption energy can be observed when the pyridyl moiety is replaced by the more conjugated isoquinoline group in complexes **14** and **15**. This is ascribed to the stabilization of the π^* orbital by the better delocalization over the C[^]N ligand upon introduction of the isoquinoline moiety, which results in a narrowing of the π - π^* energy gap.

Luminescence spectroscopy: This class of gold(III) compounds was found to exhibit rich luminescence. Their photoluminescence properties in dichloromethane solution at room temperature and in ethanol/methanol/dichloromethane (40:10:1 v/v) glass at 77 K have been studied. In dichloromethane solutions at 298 K, the gold(III) complexes exhibit intense luminescence over a broad range of wavelengths covering 462–697 nm at room temperature. The photophysical data of **1–15** are tabulated in Table 4. In contrast

to the dichlorogold(III) precursor complexes, $[\text{Au}(\text{C}^{\wedge}\text{N})\text{Cl}_2]$, which is reported to be non-emissive at room temperature and is only emissive at low-temperature glass,^[10] incorporation of the strong electron-donating alkynyl ligands into gold(III) has led to the enhancement of the photoluminescence properties of these cyclometalated gold(III) complexes through the enlargement of the d-d ligand-field splitting. This concept has also been demonstrated in other related organogold(III) complexes, $[\text{Au}(\text{RC}^{\wedge}\text{N}^{\wedge}\text{CR})(\text{C}\equiv\text{C}-\text{R})]^{[8]}$ and $[\text{Au}_n(\text{RC}^{\wedge}\text{N}^{\wedge}\text{CR})_n(\text{NHC})]^{n+}$ ($n=1-2$).^[9] Figure 4a depicts the emission spectra of **1**, **11**, **14**, and **15** in dichloromethane solution at room temperature. The emission lifetimes in the sub-microsecond to microsecond range, together with the observed large Stokes shifts, suggest that the emission is of triplet parentage.

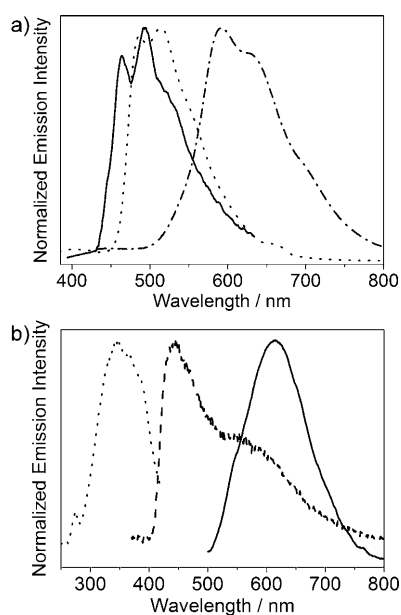


Figure 4. a) Emission spectra of **1** (—), **11** (.....), and **15** (---) in degassed CH_2Cl_2 at room temperature; b) Excitation spectrum (.....), and emission spectra with excitation wavelength at 350 nm (----) and 450 nm (—) of **4** in degassed CH_2Cl_2 at room temperature.

Upon excitation at $\lambda \geq 320$ nm, complexes **1–3** and **5**, which contain the same unsubstituted ppy ligand, exhibit nearly identical emission spectra, in which a vibronic-structured emission band with a band maximum at approximately 464 nm was observed. The same behavior was also observed for complexes **6–8** that contain the same 2-(*p*-tolyl)pyridine (ptpy) ligand, with band maximum at approximately 473 nm. This suggests that the emission energies of the complexes are rather insensitive to the nature of the alkynyl ligands. The vibrational progressional spacings of about 1200–1300 cm^{-1} are characteristic of the C=C and C=N stretching modes of the cyclometalating C[^]N ligand, indicative of the involvement of the C[^]N ligand in the excited-state origin. The luminescence is assigned as originating from a metal-perturbed $^3[\pi-\pi^*(\text{C}^{\wedge}\text{N})]$ IL state, with some charge-transfer

character from the aryl ring to the pyridyl moiety. Similar assignment has also been made in the related bis-cyclometalated alkynylgold(III) complexes.^[8] Similar to the electronic absorption study, attachment of the electron-donating methyl, *tert*-butyl and methoxy groups on the phenyl rings of the ppy ligand has resulted in lower-energy emission bands in complexes **6–13** when compared with complexes **1–3** and **5** with the unsubstituted ppy ligand, due to the reduction in $\pi-\pi^*$ energy separation of the C[^]N ligand. Variation of the substituents on the aryl and the pyridyl rings on the C[^]N ligands can lead to the tuning of the emission energies of the dialkynylgold(III) complexes, as demonstrated by complexes **10–13**, which all contain the same methoxy substituent at the 4'-position of the aryl ring but different substituents on the pyridyl ring. Compared with complex **10**, complex **13** shows an obvious red shift in emission energy because of the presence of a strongly electron-withdrawing trifluoromethyl substituent at the 5-position of the pyridyl ring, which lowers the pyridyl-based LUMO π^* orbital to a larger extent than the aryl-based HOMO π orbital, giving rise to a narrower $\pi-\pi^*$ energy gap. On the other hand, attachment of an electron-donating methyl substituent at the 4-position of the pyridyl ring in complex **12** resulted in an increase in the energy level of the LUMO π^* orbital, leading to a wider $\pi-\pi^*$ energy gap and therefore a blue shift in emission relative to complex **10**. The presence of the less strongly electron-donating methyl group at the 5-position of the pyridyl ring, on the contrary, will cause a slight red shift in the emission energy. The same observation has also been observed in a series of diketonoplatinum(II) complexes containing ppy ligands with substituents at different positions of the aryl and pyridyl rings reported by Thompson and co-workers, with results supported by density functional theory (DFT) calculations.^[18] According to the DFT study on the related $[\text{Pt}(\text{acac})(\text{R}-\text{ppy})]$ system,^[18] the HOMO and LUMO of all the complexes are of similar nature. The HOMO is aryl based, and a large amount of electron density is centered at the 5'-position of the phenyl ring with nodes at the 4'- and 6'- positions; whereas the pyridyl ring of the LUMO contains the majority of its electron density, with large amounts of electron density centered at the 4-position and nodes at the 5- and 6-positions.^[18] Therefore, the red shift in complex **12** relative to complex **10** is attributed to the attachment of the less strongly electron-donating methyl substituent at the node of the pyridyl-based LUMO.

To reduce the $\pi-\pi^*$ energy gap to lower the emission energy further, the more conjugated phenylisoquinoline-type ligands were employed in complexes **14** and **15**. This resulted in a dramatic shift of emission maximum from 464 nm in complex **1** to 582 nm in complex **14** and 592 nm in complex **15**. This can be explained by the fact that the isoquinoline-based LUMO (π^* orbital) is stabilized to a much larger extent than the phenyl-based HOMO (π orbital) due to the increase in conjugation. As a consequence, the $\pi-\pi^*$ energy gap is narrower than the case in the complexes with ppy-type ligands, contributing to lower emission energies for complex **14**. The further reduction in emission energy in **15**

was attributed to the attachment of the strongly electron-donating methoxy group on the aryl ring of the C[^]N ligand.

Unlike other members of this series of dialkynylgold(III) complexes, which generally show a vibronic-structured emission band in dichloromethane solution under ambient conditions, complex **4** with an electron-rich aminophenyl alkynyl group showed a low-energy structureless emission band centered at approximately 613 nm as well as an intraligand emission band centered at 441 nm. The excitation and emission spectra of complex **4** are shown in Figure 4b. The low-energy structureless emission band is tentatively assigned as being derived from an excited state of ³LLCT [$\pi(\text{C}\equiv\text{CC}_6\text{H}_4\text{NH}_2)\rightarrow\pi^*(\text{C}^{\wedge}\text{N})$] origin mixed with some ³IL [$\pi\rightarrow\pi^*(\text{C}^{\wedge}\text{N})$] states, because the presence of the strong electron-donating amino substituent will render the $\pi(\text{C}\equiv\text{CC}_6\text{H}_4\text{NH}_2)$ orbital more high lying in energy. Such an assignment is in accordance with related bis-cyclometalated alkynylgold(III) complexes containing amino-, dimethylamino-, and diphenylaminoalkynyl ligands.^[8] In addition to the LLCT emission at approximately 613 nm, a metal-perturbed intraligand emission band could also be observed at approximately 441 nm for complex **4**. The excitation spectra monitored at both wavelengths were found to give the same excitation spectra. Hence it is expected that the intraligand state and the LLCT state of complex **4** lie very close in energy, such that when the complex was excited at higher energy, dual luminescence from both IL and LLCT origins could be observed. However, when the complex was excited at lower energy at 430 nm or longer wavelengths, only the LLCT band could be observed. Furthermore, note that the photoluminescence quantum yields of this class of complexes, which are in the range $1.3\text{--}10.3\times 10^{-2}$, are comparatively higher than those of the related bis-cyclometalated alkynylgold(III) complexes (with Φ_{lum} in the order of $\times 10^{-3}$).^[8]

For emission studies in low-temperature glasses, all of the complexes showed vibronic-structured emission bands with emission energies similar to those observed in dichloromethane solution. The emission spectra of **4**, **13**, and **15** in low-temperature EtOH/MeOH/CH₂Cl₂ (40:10:1 v/v) glass at 77 K are shown in Figure 5. These emission bands were similarly assigned as derived from intraligand states of the cyclometalating C[^]N ligand. As in dichloromethane solution, the

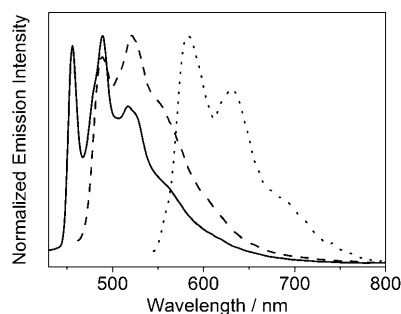


Figure 5. Emission spectra of **4** (—), **13** (----), and **15** (.....) in a low-temperature EtOH/MeOH/CH₂Cl₂ (40:10:1 v/v) glass at 77 K.

ethanol/methanol/dichloromethane glass emission also exhibited vibrational progression spacings of 1200–1400 cm⁻¹, which agree well with the C=C and C=N stretching modes of the C[^]N ligands. This is also in agreement with the low-temperature emission of the dichlorogold(III) complex, [Au(ppy)Cl₂], previously reported in the literature.^[10,11] Note that the emission spectrum of complex **4** in the 77 K glass also exhibited a similar vibronic-structured emission band, in contrast to that recorded in dichloromethane solution, in which a structureless emission band was observed. The change of emission origin in **4** from the ³LLCT [$\pi(\text{C}\equiv\text{CC}_6\text{H}_4\text{NH}_2)\rightarrow\pi^*(\text{C}^{\wedge}\text{N})$] excited state to the metal-perturbed ³IL [$\pi\rightarrow\pi^*(\text{C}^{\wedge}\text{N})$] excited state by a lowering of the medium temperature indicates that these two excited states lie relatively close in energy.

Nanosecond UV/Vis transient absorption (TA) spectroscopy:

To obtain more information on the nature of the excited states, nanosecond TA measurements were performed on complexes **1** and **4** in degassed dichloromethane solution. The measurements were conducted at 288 K to minimize any side reactions and/or decompositions that might occur upon laser excitation. The TA difference spectra of **1** and **4** determined at different delay times after a 355 nm laser pulse are shown, respectively, in Figure 6 and Figure 7. For complex **1**, the TA spectrum features two bands, an intense broad band in the 355–455 nm region and a weaker absorption band at approximately 488 nm. These transient signals were found to decay monoexponentially with a lifetime of

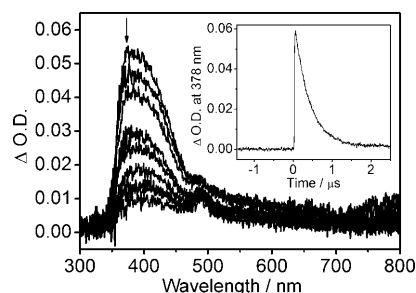


Figure 6. Transient absorption spectra of **1** in CH₂Cl₂ at 288 K at decay times of 0–0.8 μs (at intervals of 0.1 μs). Inset shows the decay trace of the absorptions at 378 nm.

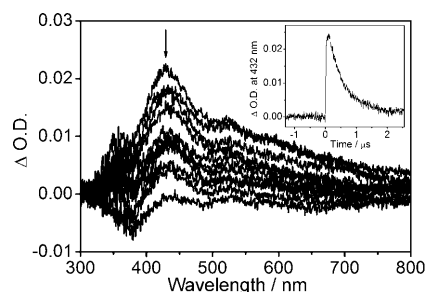


Figure 7. Transient absorption spectra of **4** in CH₂Cl₂ at 288 K at decay times of 0–1 μs (at intervals of 0.1 μs). Inset shows the decay trace of the absorption at 432 nm.

0.38 μ s. Given the longer decay time of the transient signals than the emission decay, the intense TA band in the 355–455 nm region could not be assigned as the triplet excited state absorption of the complex. Instead, the band at 355–455 nm was assigned to the absorption of the anion radical of the ppy ligand because similar assignment has been made for Ir^{III} complexes containing ppy and the related 2,2'-bipyridyl (bpy) ligand.^[19] The lower-energy band at approximately 488 nm was tentatively assigned as the absorption of the radical cation of the 4-methoxyphenyl alkynyl ligand, given its close resemblance to that observed for the radical cations of the related anisole as well as various dimethoxy- and trimethoxy-substituted benzenes and phenols (>400 nm).^[20,21] Thus, it is believed that upon excitation of the ground state, an intraligand triplet state was initially formed, which readily underwent facile charge separation to give the [(ppy⁻)Au^{III}(C \equiv CC₆H₄OMe⁺)] charge-separated state.

Similarly, the TA difference spectrum of complex **4** was characterized by an intense positive absorption band centered at approximately 432 nm and a weaker positive absorption band centered at approximately 525 nm that decayed monoexponentially with a lifetime of 0.45 μ s. Similar to the case for complex **1**, the absorption at approximately 432 nm is characteristic of the absorption of the ppy radical anion, whereas the weaker, broad TA band centered at approximately 525 nm is tentatively assigned as the 4-aminophenylalkynyl radical cation absorption. A similar TA band has also been observed for the radical cation of free 4-aminophenylacetylene^[22] and the related aniline and chloroaniline molecules.^[23] The transient absorptions are tentatively assigned as the absorption of the [(ppy⁻)Au^{III}(C \equiv C-C₆H₄NH₂⁺)] charge-separated state, which is formed after the population of the initial triplet excited state and has a charge-recombination rate constant of 2.23×10^6 s⁻¹.

Conclusion

A novel class of luminescent dialkynylgold(III) complexes has been synthesized and characterized. The X-ray crystal structures of **1**, **6**, **11**, **12**, and **15** have been determined. Electrochemical studies reveal the presence of a ligand-centered reduction originating from the cyclometalating C^N ligand, whereas the first oxidation wave is associated with an alkynyl ligand-centered oxidation. The electronic absorption and emission properties of the complexes have also been studied. In dichloromethane solution at room temperature, the low-energy absorption bands are ascribed to the intraligand π - π^* transition, with mixing of a charge-transfer character from the aryl ring to the pyridine or isoquinoline moiety of the cyclometalating C^N ligand. For the emission studies in dichloromethane solution at room temperature and in low-temperature glass, vibronic-structured emission bands were observed, with the exception of complex **4**, which are tentatively assigned as originating from intraligand π - π^* states with aryl-to-pyridine or isoquinoline charge-transfer character of the cyclometalating C^N

ligand. Complex **4**, on the other hand, showed a structureless emission band originating from the ³LLCT [π (C \equiv CC₆H₄NH₂) \rightarrow π^* (C^N)] excited state. The excited-state properties of complexes **1** and **4** have also been studied by TA spectroscopy. The photophysical properties of this class of complexes can be readily tuned by the variation of the cyclometalating C^N ligand, and the alkynyl ligands are thought to play an important role in the enhancement of luminescence properties of the gold(III) complexes.

Experimental Section

Materials and reagents: Potassium tetrachloroaurate(III) was purchased from ChemPur. Tetra-*n*-butylammonium hexafluorophosphate was obtained from Strem Inc. The dichlorogold(III) precursor complex, [Au(ppy)Cl₂], was prepared according to a reported procedure.^[12] All other dichlorogold(III) precursors, [Au(C^N)Cl₂], were prepared by using the same methodology, with different cyclometalating C^N ligands used in place of ppy. 2-Phenylpyridine and 2-(*p*-tolyl)pyridine were purchased from Sigma-Aldrich, whereas other C^N ligands were prepared from 2-bromopyridine or 1-chloroisoquinoline by using the respective boronic acids by the standard Suzuki coupling procedure.^[13] *n*-Butyllithium (1.6 M in hexanes) was purchased from Acros, whereas 4-methoxyphenylacetylene, 4-*n*-butylphenylacetylene, 4-ethylphenylacetylene, and 4-(trifluoromethyl)phenylacetylene were from Sigma-Aldrich. 4-Aminophenylacetylene was prepared according to a reported procedure.^[24] All solvents were purified and distilled by using standard procedures before use. All other reagents were of analytical grade and were used as received. Tetra-*n*-butylammonium hexafluorophosphate (Aldrich) was recrystallized twice from absolute ethanol before use.

Physical measurements and instrumentation: UV/Vis spectra were obtained on a Hewlett-Packard 8452 A diode array spectrophotometer. ¹H NMR spectra were recorded on a Bruker DPX-300 (300 MHz) or Bruker DPX-400 (400 MHz) Fourier transform NMR spectrometer with chemical shifts recorded relative to tetramethylsilane (Me₄Si). Positive FAB mass spectra were recorded on a Finnigan MAT95 mass spectrometer. Elemental analyses for the metal complexes were performed on the Carlo Erba 1106 elemental analyzer at the Institute of Chemistry, Chinese Academy of Sciences (Beijing, China). Steady-state excitation and emission spectra were recorded on a Spex Fluorolog-2 model F111 fluorescence spectrofluorometer equipped with a Hamamatsu R-928 photomultiplier tube. Photophysical measurements in low-temperature glasses were carried out with the sample solution loaded in a quartz tube inside a quartz-walled Dewar flask. Liquid nitrogen was placed into the Dewar flask for low-temperature (77 K) photophysical measurements. Excited-state lifetimes of solution samples were measured by using a conventional laser system. The excitation source used was the 355 nm output (third harmonic, 8 ns) of a Spectra-Physics Quanta-Ray Q-switched GCR-150 pulsed Nd:YAG laser (10 Hz). Luminescence quantum yields were measured by the optical dilute method reported by Demas and Crosby.^[25a] A degassed aqueous solution of quinine sulfate in sulfuric acid (1.0 N) ($\Phi = 0.546$, excitation wavelength at 365 nm) was used as the reference and corrected for the refractive index of the solution.^[25b] TA measurements were performed on a LP920-KS Laser Flash Photolysis Spectrometer (Edinburgh Instruments Ltd, Livingston, UK) at ambient temperature. The excitation source was the 355 nm output (third harmonic) of a Nd:YAG laser and the probe light source was a Xe900 450W xenon arc lamp. The TA spectra were detected by an image-intensified CCD camera (Andor) with a PC plug-in controller, fully operated by L900 spectrometer software. The absorption kinetics were detected by a Hamamatsu R928 photomultiplier tube and recorded on a Tektronix Model TDS3012B (100 MHz, 1.25 GS⁻¹) digital oscilloscope and were analyzed by using the same software for exponential-fit analysis (tail-fit data analysis). All solution samples for photophysical studies were freshly prepared under a high vacuum in a 10 cm³ round-bottomed flask equipped with a

sidearm 1 cm fluorescence cuvette and were sealed from the atmosphere by a Rotaflo HP6/6 quick-release Teflon stopper. Solutions were rigorously degassed on a high-vacuum line in a two-compartment cell with no less than four successive freeze-pump-thaw cycles. Cyclic voltammetric measurements were performed by using a CH Instruments model CHI 600 A electrochemical analyzer. The electrolytic cell used was a conventional two-compartment cell. Electrochemical measurements were performed in dichloromethane solutions with TBAH (0.1 M) as the supporting electrolyte at room temperature. The reference electrode was a Ag/AgNO₃ (0.1 M in acetonitrile) electrode, and the working electrode was a glassy carbon electrode (CH Instruments) with a platinum wire as the counter electrode. The working electrode surface was first polished with a 1 μm alumina slurry (Linde), followed by a 0.3 μm alumina slurry, on a microcloth (Buehler). Treatment of the electrode surfaces was as reported previously.^[26a] The ferrocenium/ferrocene couple (FcCp^{+/0}) was used as the internal reference.^[26b] All solutions for electrochemical studies were deaerated with prepurified argon gas just before measurements.

Crystal-structure determination: Single crystals of **1**, **6**, **11**, **12**, and **15** suitable for X-ray diffraction studies were grown by layering of *n*-hexane onto a concentrated dichloromethane solution of the respective complexes. The X-ray diffraction data were collected on a Bruker Smart CCD 1000 using graphite-monochromatized MoK_α radiation (λ = 0.71073 Å). The images were interpreted and intensities were integrated by using the DENZO program.^[27] The structure was solved by direct methods employing the SHELXS-97 program.^[28] Full-matrix least-squares refinement on *F*² was used in the structure refinement. The positions of H atoms were calculated based on the riding mode with thermal parameters equal to 1.2 times those of the associated C atoms and participated in the calculation of final *R*-indices. In the final stage of the least-squares refinement, all non-hydrogen atoms were refined anisotropically. CCDC-783733 (**1**), CCDC-783734 (**6**), CCDC-783735 (**11**), CCDC-783736 (**12**), and CCDC-783737 (**15**) contain the supplementary crystallographic data for this paper. These data can be obtained free of charge from The Cambridge Crystallographic Data Centre via www.ccdc.cam.ac.uk/data_request/cif.

Synthesis

General procedure for syntheses of dialkynylgold(III) complexes: *n*-Butyllithium (1.44 mmol, 1.6 M in hexanes) was added to a solution of alkyne (1.20 mmol) in tetrahydrofuran (20 mL) under a nitrogen atmosphere in a dropwise manner at -78 °C. The resulting mixture was stirred for 5 min and transferred to a suspension of [Au(C[^]N)Cl₂] (0.30 mmol) in tetrahydrofuran (30 mL). The reaction mixture was stirred for 3 h at room temperature. The crude product, which was obtained upon removal of solvent from the reaction mixture, was subjected to purification by column chromatography on silica gel by using dichloromethane as the eluent. Subsequent recrystallization by slow diffusion of diethyl ether vapor into the concentrated dichloromethane solution of the compound gave the resulting complex as yellow to orange crystals.

[Au(ppy)(C≡C-C₆H₄-OCH₃-p)₂] **1**: Complex **1** was prepared from [Au(ppy)Cl₂] (127 mg) and 4-methoxyphenylacetylene (159 mg) according to the general procedure and was obtained as yellow crystals (yield: 61 mg, 33%). ¹H NMR (400 MHz, CDCl₃, 298 K): δ = 3.82 (s, 6H; -OCH₃), 6.85 (m, 4H; -C₆H₄-), 7.39 (m, 1H; ppy), 7.41 (m, 2H), 7.50–7.56 (m, 4H; -C₆H₄-), 7.67 (d, *J* = 5.7 Hz, 1H; ppy), 7.90 (d, *J* = 6.0 Hz, 1H; ppy), 8.06 (t, *J* = 6.5 Hz, 1H; ppy), 8.30 (d, *J* = 7.5 Hz, 1H; ppy), 9.71 ppm (d, *J* = 4.8 Hz, 1H; ppy); IR (KBr): $\tilde{\nu}$ = 2120, 2167 cm⁻¹ ($\tilde{\nu}$ (C≡C)); positive FABMS: *m/z*: 614 [M]⁺; elemental analysis calcd (%) for C₂₉H₂₂NO₂Au: C 56.78, H 3.61, N 2.28; found: C 56.94, H 3.87, N 2.32.

[Au(ppy)(C≡C-C₆H₄-C₂H₅-p)₂] **2**: Complex **2** was prepared from [Au(ppy)Cl₂] (127 mg) and 4-ethylphenylacetylene (156 mg) according to the general procedure and was obtained as yellow crystals (yield: 51 mg, 28%). ¹H NMR (400 MHz, CDCl₃, 298 K): δ = 1.24 (s, 6H; -CH₃), 2.65 (m, 4H; -CH₂-), 7.14 (m, 4H; -C₆H₄-), 7.38 (m, 3H; ppy), 7.51 (m, 4H; -C₆H₄-), 7.66 (d, *J* = 7.0 Hz, 1H; ppy), 7.89 (m, 1H; ppy), 8.04 (s, 1H; ppy), 8.27 (d, *J* = 7.0 Hz, 1H; ppy), 9.67 ppm (s, 1H; ppy); IR (KBr): $\tilde{\nu}$ = 2136, 2163 cm⁻¹ ($\tilde{\nu}$ (C≡C)); positive FABMS: *m/z*: 609 [M]⁺; elemental analysis calcd (%) for C₃₁H₂₆NAu·1/2C₃H₁₂: C 62.32, H 5.00, N 2.17; found: C 62.31, H 4.60, N 2.52.

[Au(ppy)(C≡C-C₆H₄-CF₃-p)₂] **3**: Complex **3** was prepared from [Au(ppy)Cl₂] (127 mg) and 4-trifluoromethylphenylacetylene (204 mg) according to the general procedure and was obtained as orange crystals (yield: 58 mg, 28%). ¹H NMR (400 MHz, CD₂Cl₂, 298 K): δ = 7.40 (m, 2H; ppy), 7.48 (m, 1H; ppy), 7.57 (m, 4H; -C₆H₄-), 7.65 (m, 4H; -C₆H₄-), 7.66 (m, 1H; ppy), 7.94 (d, 8.1 Hz, 1H; ppy), 8.09 (dt, *J* = 1.3 and 7.3 Hz, 1H; ppy), 8.17 ppm (dd, *J* = 1.3 and 7.3 Hz; ppy); IR (KBr): $\tilde{\nu}$ = 2136, 2166 cm⁻¹ ($\tilde{\nu}$ (C≡C)); positive FABMS: *m/z*: 689 [M]⁺; elemental analysis calcd (%) for C₂₉H₁₆NF₃Au: C 50.52, H 2.34, N 2.03; found: C 50.35, H 2.36, N 2.08.

[Au(ppy)(C≡C-C₆H₄-NH₂-p)₂] **4**: Complex **4** was prepared from [Au(ppy)Cl₂] (127 mg) and 4-aminophenylacetylene (141 mg) according to the general procedure and was obtained as dark-orange crystals (yield: 96 mg, 55%). ¹H NMR (400 MHz, [D₆]DMSO, 298 K): δ = 5.24 (s, 2H; -NH₂), 5.30 (s, 2H; -NH₂), 6.56 (m, 4H; -C₆H₄-), 7.17 (dd, *J* = 2.5 and 5.6 Hz, 4H; -C₆H₄-), 7.41 (m, 2H; ppy), 7.75 (m, 1H; ppy), 8.01 (d, *J* = 7.6 Hz, 1H; ppy), 8.16 (d, *J* = 7.6 Hz, 1H; ppy), 8.34 (m, 2H; ppy), 9.57 ppm (d, *J* = 5.6 Hz, ppy); IR (KBr): $\tilde{\nu}$ = 2129, 2191 cm⁻¹ ($\tilde{\nu}$ (C≡C)); positive FABMS: *m/z*: 584 [M]⁺; elemental analysis calcd (%) for C₂₇H₂₀N₃Au·1/2H₂O: C 54.74, H 3.57, N 7.09; found: C 54.81, H 3.40, N 7.09.

[Au(ppy)(C≡C-Si(CH₃)₃)₂] **5**: Complex **5** was prepared from [Au(ppy)Cl₂] (127 mg) and trimethylsilylacetylene (118 mg) according to the general procedure and was obtained as pale-yellow crystals (yield: 20 mg, 12%). ¹H NMR (400 MHz, CD₂Cl₂, 298 K): δ = 0.23 (s, 9H; -Si(CH₃)₃), 0.25 (s, 9H; -Si(CH₃)₃), 7.31–7.43 (m, 3H; ppy), 7.69 (dd, *J* = 1.4 and 7.5 Hz, 1H; ppy), 7.91 (d, *J* = 8.1 Hz, 1H; ppy), 8.06 (m, 1H; ppy), 8.13 (dd, *J* = 1.4 and 7.5 Hz, 1H; ppy), 9.58 ppm (d, *J* = 5.7 Hz, 1H; ppy); IR (KBr): $\tilde{\nu}$ = 2075, 2098 cm⁻¹ ($\tilde{\nu}$ (C≡C)); positive FABMS: *m/z*: 546 [M]⁺; elemental analyses calcd (%) for C₂₁H₂₆NSi₂Au·1/2H₂O: C 45.48, H 4.71, N 2.67; found: C 45.12, H 4.91, N 2.53.

[Au(pty)(C≡C-C₆H₄-OCH₃-p)₂] **6**: Complex **6** was prepared from [Au(pty)Cl₂] (131 mg) and 4-methoxyphenylacetylene (159 mg) according to the general procedure and was obtained as yellow crystals (yield: 96 mg, 60%). ¹H NMR (300 MHz, CDCl₃, 298 K): δ = 2.41 (s, 3H; -CH₃), 3.82 (s, 6H; -OCH₃), 6.85 (m, 4H; -C₆H₄-), 7.14 (d, *J* = 7.9 Hz, 1H; pty), 7.36 (t, *J* = 7.2 Hz, 1H; pty), 7.57–7.37 (m, 5H; pty and -C₆H₄-), 7.83 (d, *J* = 8.0 Hz, 1H; pty), 7.99 (t, 7.5 Hz, 1H; pty), 8.11 (s, 1H; pty), 9.66 ppm (d, *J* = 5.7 Hz, 1H; pty); IR (KBr): $\tilde{\nu}$ = 2130, 2163 cm⁻¹ ($\tilde{\nu}$ (C≡C)); positive FABMS: *m/z*: 532 [M]⁺; elemental analysis calcd (%) for C₃₆H₃₄NO₂Au·1/2CH₃OH: C 56.93, H 4.07, N 2.18; found: C 56.90, H 3.87, N 2.31.

[Au(pty)(C≡C-C₆H₄-C₄H₉-p)₂] **7**: Complex **7** was prepared from [Au(pty)Cl₂] (131 mg) and 4-*n*-butylphenylacetylene (190 mg) according to the general procedure and was obtained as yellow crystals (yield: 61 mg, 39%). ¹H NMR (400 MHz, CD₂Cl₂, 298 K): δ = 0.94 (m, 6H; -CH₃), 1.38 (m, 4H; -CH₂-), 1.59 (m, 4H; -CH₂-), 2.38 (s, 3H; -CH₃), 2.61 (m, 4H; -CH₂-), 7.15 (m, 5H; pty and -C₆H₄-), 7.36 (m, 1H; pty), 7.43 (dd, *J* = 8.1 and 4.7 Hz, 4H; -C₆H₄-), 7.58 (d, *J* = 8.1 Hz, 1H; pty), 7.85 (d, *J* = 8.1 Hz, 1H; pty), 7.99 (m, 2H; pty), 9.57 ppm (dd, *J* = 1.1 and 4.7 Hz, 1H; pty); IR (KBr): $\tilde{\nu}$ = 2113, 2167 cm⁻¹ ($\tilde{\nu}$ (C≡C)); positive FABMS: *m/z*: 522 [M-C≡CC₆H₄-C₄H₉]⁺; elemental analysis calcd (%) for C₃₆H₃₆NAu: C 63.62, H 5.34, N 2.06; found: C 63.80, H 5.56, N 2.29.

[Au(pty)(C≡C-Si(CH₃)₃)₂] **8**: Complex **8** was prepared from [Au(pty)Cl₂] (131 mg) and trimethylsilylacetylene (118 mg) according to the general procedure and was obtained as pale-yellow crystals (yield: 25 mg, 15%). ¹H NMR (400 MHz, CD₂Cl₂, 298 K, relative to Me₄Si): δ = 0.23 (s, 9H; -Si(CH₃)₃), 0.27 (s, 9H; -Si(CH₃)₃), 2.37 (s, 3H; -CH₃), 7.14 (d, *J* = 7.9 Hz, 1H; ppy), 7.35 (t, *J* = 6.1 Hz, 1H; ppy), 7.57 (d, *J* = 7.9 Hz, 1H; ppy), 7.84 (d, *J* = 7.9 Hz, 1H; ppy), 7.97 (s, 1H; ppy), 8.02 (m, 1H; ppy), 9.54 ppm (d, *J* = 4.9 Hz, 1H; ppy); IR (KBr): $\tilde{\nu}$ = 2075, 2098 cm⁻¹ ($\tilde{\nu}$ (C≡C)); positive FABMS: *m/z*: 560 [M]⁺; elemental analysis calcd (%) for C₂₂H₂₈NSi₂Au·1/2H₂O: C 46.47, H 5.14, N 2.46; found: C 46.50, H 5.07, N 2.46.

[Au(tbppy)(C≡C-C₆H₄-OCH₃-p)₂] (tbppy = 2-(*p*-*tert*-butyl)phenyl)pyridine) **9**: Complex **9** was prepared from [Au(tbppy)Cl₂] (143 mg) and 4-methoxyphenylacetylene (159 mg) according to the general procedure and was obtained as orange crystals (yield: 42 mg, 21%). ¹H NMR

(300 MHz, CD₂Cl₂, 298 K): δ = 1.36 (s, 9H; *t*Bu), 3.80 (s, 6H; -OCH₃), 6.86 (m, 4H; -C₆H₄-), 7.40 (m, 2H; *tbppy*), 7.48 (m, 4H; -C₆H₄-), 7.65 (d, J = 8.2 Hz, 1H; *tbppy*), 7.89 (d, J = 7.9 Hz, 1H; *tbppy*), 8.02 (t, J = 7.9 Hz, 1H; *tbppy*), 8.38 (d, J = 1.9 Hz, 1H; *tbppy*), 9.64 ppm (d, J = 5.0 Hz; *tbppy*); IR (KBr): $\tilde{\nu}$ = 2098, 2143 cm⁻¹ ($\tilde{\nu}$ (C≡C)); positive FABMS: m/z : 669 [M]⁺; elemental analysis calcd (%) for C₃₃H₃₀NO₂Au^{1/2}H₂O: C 58.41, H 4.60, N 2.06; found: C 58.36, H 4.60, N 1.99.

[Au(*mppy*)(C≡C-C₆H₄-OCH₃-*p*)] (*mppy* = 2-(*p*-methoxyphenyl)pyridine) **10**: Complex **10** was prepared from [Au(*mppy*)Cl₂] (136 mg) and 4-methoxyphenylacetylene (159 mg) according to the general procedure and was obtained as orange crystals (yield: 27 mg, 14%). ¹H NMR (300 MHz, CD₂Cl₂, 298 K): δ = 3.80 (s, 6H; -OCH₃), 3.87 (s, 3H; -CH₃), 6.85 (m, 5H; -C₆H₄- and *mppy*), 7.33 (t, J = 7.8 Hz, 1H; *mppy*), 7.47 (m, 4H; -C₆H₄-), 7.68 (d, J = 7.8 Hz, 1H; *mppy*), 7.78 (d, J = 7.8 Hz, 1H; *mppy*), 7.85 (d, J = 2.6 Hz, 1H; *mppy*), 8.00 (t, J = 7.8 Hz, 1H; *mppy*), 9.56 ppm (m, 1H; *mppy*); IR (KBr): $\tilde{\nu}$ = 2131, 2162 cm⁻¹ ($\tilde{\nu}$ (C≡C)); positive FABMS: m/z : 643 [M]⁺; elemental analysis calcd (%) for C₃₀H₂₄AuNO₃^{1/2}H₂O: C 55.22, H 3.86, N 2.15; found: C 55.42, H 3.82, N 2.19.

[Au(*mpmepy*)(C≡C-C₆H₄-OCH₃-*p*)] (*mpmepy* = 5-methyl-2-(*p*-methoxyphenyl)pyridine) **11**: Complex **11** was prepared from [Au(*mpmepy*)Cl₂] (140 mg) and 4-methoxyphenylacetylene (159 mg) according to the general procedure and was obtained as orange crystals (yield: 59 mg, 30%). ¹H NMR (300 MHz, CD₂Cl₂, 298 K): δ = 2.40 (s, 3H; -CH₃), 3.80 (s, 6H; -OCH₃), 3.85 (s, 3H; -OCH₃), 6.85 (m, 5H; *mpmepy* and -C₆H₄-), 7.49 (m, 4H; -C₆H₄-), 7.64 (q, J = 8.3 Hz, 2H; *mpmepy*), 7.81 (m, 2H; *mpmepy*), 9.40 ppm (s, 1H; *mpmepy*); IR (KBr): $\tilde{\nu}$ = 2132, 2161 cm⁻¹ ($\tilde{\nu}$ (C≡C)); positive FABMS: m/z : 657 [M]⁺; elemental analysis calcd (%) for C₃₁H₂₆NO₃Au^{1/2}H₂O: C 55.86, H 4.08, N 2.10; found: C 55.85, H 3.94, N 2.21.

[Au(4-*mpmepy*)(C≡C-C₆H₄-OCH₃-*p*)] (4-*mpmepy* = 4-methyl-2-(*p*-methoxyphenyl)pyridine) **12**: Complex **12** was prepared from [Au(4-*mpmepy*)Cl₂] (140 mg) and 4-methoxyphenylacetylene (159 mg) according to the general procedure and was obtained as orange crystals (yield: 51 mg, 26%). ¹H NMR (300 MHz, CD₂Cl₂, 298 K): δ = 2.50 (s, 3H; -CH₃), 3.80 (s, 6H; -OCH₃), 3.86 (s, 3H; -OCH₃), 6.85 (m, 5H; -C₆H₄- and 4-*mpmepy*), 7.12 (d, J = 6.1 Hz, 1H; 4-*mpmepy*), 7.46 (m, 4H; -C₆H₄-), 7.56 (s, 1H; 4-*mpmepy*), 7.64 (d, J = 8.7 Hz, 1H; 4-*mpmepy*), 7.82 (d, J = 2.7 Hz, 1H; 4-*mpmepy*), 9.35 ppm (d, J = 6.1 Hz, 1H; 4-*mpmepy*); IR (KBr): $\tilde{\nu}$ = 2129, 2160 cm⁻¹ ($\tilde{\nu}$ (C≡C)); positive FABMS: m/z : 657 [M]⁺; elemental analysis calcd (%) for C₃₀H₂₄NO₂Au^{1/2}H₂O: C 56.61, H 3.96, N 2.20; found: C 56.26, H 4.09, N 2.22.

[Au(*mptfpy*)(C≡C-C₆H₄-OCH₃-*p*)] (*mptfpy* = 5-trifluoromethyl-2-(*p*-methoxyphenyl)pyridine) **13**: Complex **13** was prepared from [Au(*mptfpy*)Cl₂] (156 mg) and 4-methoxyphenylacetylene (159 mg) according to the general procedure and was obtained as orange crystals (yield: 47 mg, 22%). ¹H NMR (300 MHz, CD₂Cl₂, 298 K): δ = 3.80 (s, 6H; -OCH₃), 3.88 (s, 3H; -OCH₃), 6.84–6.91 (m, 5H; -C₆H₄- and *mptfpy*), 7.43–7.50 (m, 4H; -C₆H₄-), 7.75 (d, J = 8.5 Hz, 1H; *mptfpy*), 7.82 (d, J = 2.6 Hz, 1H; *mptfpy*), 7.90 (d, J = 7.9 Hz, 1H; *mptfpy*), 8.17 (d, J = 8.5 Hz, 1H; *mptfpy*), 9.96 ppm (s, 1H; *mptfpy*); IR (KBr): $\tilde{\nu}$ = 2138, 2161 cm⁻¹ ($\tilde{\nu}$ (C≡C)); positive FABMS: m/z : 712 [M]⁺; elemental analysis calcd (%) for C₃₁H₂₃NO₃F₃Au^{1/2}CH₂Cl₂: C 50.18, H 3.21, N 1.86; found: C 50.35, H 3.14, N 1.97.

[Au(*piq*)(C≡C-C₆H₄-OCH₃-*p*)] (*piq* = 1-phenylisoquinoline) **14**: Complex **14** was prepared from [Au(*piq*)Cl₂] (142 mg) and 4-methoxyphenylacetylene (159 mg) according to the general procedure and was obtained as orange crystals (yield: 72 mg, 36%). ¹H NMR (300 MHz, CD₂Cl₂, 298 K): δ = 3.80 (s, 6H; -OCH₃), 6.85 (m, 4H; -C₆H₄-), 7.45 (m, 6H; -C₆H₄- and *piq*), 7.77 (d, J = 6.4 Hz, 1H; *piq*), 7.84 (d, J = 8.5 Hz, 1H; *piq*), 7.91 (t, J = 6.5 Hz, 1H; *piq*), 8.00 (d, J = 8.5 Hz, 1H; *piq*), 8.24 (d, J = 7.2 Hz, 1H; *piq*), 8.39 (dd, J = 2.1 and 7.2 Hz, 1H; *piq*), 8.90 (d, J = 8.5 Hz, 1H; *piq*), 9.59 ppm (d, J = 6.4 Hz, 1H; *piq*); IR (KBr): $\tilde{\nu}$ = 2129, 2160 cm⁻¹ ($\tilde{\nu}$ (C≡C)); positive FABMS: m/z : 664 [M]⁺; elemental analysis calcd (%) for C₃₃H₂₄NO₂Au-CH₂Cl₂: C 54.56, H 3.50, N 1.87; found: C 54.99, H 3.54, N 2.27.

[Au(*mpiq*)(C≡C-C₆H₄-OCH₃-*p*)] (*mpiq* = 1-(*p*-methoxyphenyl)isoquinoline) **15**: Complexes **15** was prepared from [Au(*mpiq*)Cl₂] (151 mg) and

4-methoxyphenylacetylene (159 mg) according to the general procedure and was obtained as orange crystals (yield: 117 mg, 56%). ¹H NMR (400 MHz, CD₂Cl₂, 298 K): δ = 3.81 (s, 6H; -OCH₃), 3.92 (s, 3H; -OCH₃), 6.85 (m, 4H; -C₆H₄-), 6.92 (dd, J = 2.8 and 8.8 Hz, 1H; *mpiq*), 7.48 (m, 4H; -C₆H₄-), 7.64 (d, J = 6.8 Hz, 1H; *mpiq*), 7.78 (t, J = 6.8 Hz, 1H; *mpiq*), 7.88 (t, J = 6.8 Hz, 1H; *mpiq*), 7.94 (d, J = 7.8 Hz, 1H; *mpiq*), 8.01 (d, J = 2.8 Hz, 1H; *mpiq*), 8.20 (d, J = 9.0 Hz, 1H; *mpiq*), 8.82 (d, J = 8.8 Hz, 1H; *mpiq*), 9.48 ppm (d, J = 6.8 Hz, 1H; *mpiq*); IR (KBr): $\tilde{\nu}$ = 2129, 2162 cm⁻¹ ($\tilde{\nu}$ (C≡C)); positive FABMS: m/z : 694 [M]⁺; elemental analysis calcd (%) for C₃₄H₂₆AuNO₃^{1/2}H₂O: C 58.13, H 3.87, N 1.99; found: C 58.17, H 3.80, N 1.98.

Acknowledgements

V.W.-W.Y. acknowledges support from The University of Hong Kong under the Distinguished Research Achievement Award Scheme, the World Gold Council GROW Programme, and the URC Strategic Research Theme on Molecular Materials. This work has been supported by the University Grants Committee (UGC) Areas of Excellence Scheme (AoE/P-03/08), the UGC Special Equipment Grant (SEG_HKU07), and the Innovation and Technology Fund (ITF Tier 3 Project ITS/142/08). V.K.-M.A. acknowledges the receipt of a postgraduate studentship from The University of Hong Kong.

- [1] a) M. A. Baldo, S. Lamansky, P. E. Burrows, M. E. Thompson, S. R. Forrest, *Appl. Phys. Lett.* **1999**, *75*, 4–6; b) C. Adachi, M. A. Baldo, S. R. Forrest, M. E. Thompson, *Appl. Phys. Lett.* **2000**, *77*, 904–906; c) M. Ikai, S. Tokito, Y. Sakamoto, T. Suzuki, Y. Taga, *Appl. Phys. Lett.* **2001**, *79*, 156–158.
- [2] a) C. Adachi, R. C. Kwong, P. I. Djurovich, V. Adamovich, M. A. Baldo, M. E. Thompson, S. R. Forrest, *Appl. Phys. Lett.* **2001**, *79*, 2082–2084; b) Y. Kawamura, K. Goushi, J. Brooks, J. J. Brown, H. Sasabe, C. Adachi, *Appl. Phys. Lett.* **2005**, *86*, 071104–1–3; c) A. F. Rausch, M. E. Thompson, H. Yersin, *Inorg. Chem.* **2009**, *48*, 1928–1937.
- [3] a) A. F. Rausch, M. E. Thompson, H. Yersin, *Chem. Phys. Lett.* **2009**, *468*, 46–51; b) W. Y. Wong, Z. He, S.-K. So, K.-L. Tong, Z. Lin, *Organometallics* **2005**, *24*, 4079–4082; c) G.-J. Zhou, X.-Z. Wang, W.-Y. Wong, X.-M. Yu, H.-S. Kwok, Z. Lin, *J. Organomet. Chem.* **2007**, *692*, 3461–3473; d) G.-J. Zhou, Q. Wang, W.-Y. Wong, D. Ma, L. Wong, Z. Lin, *J. Mater. Chem.* **2009**, *19*, 1872–1883.
- [4] P. G. Bomben, B. D. Koivisto, C. P. Berlinguette, *Inorg. Chem.* **2010**, *49*, 4960–4971.
- [5] J. A. Gareth Williams, *Top. Curr. Chem.* **2007**, *281*, 205–268.
- [6] a) V. W.-W. Yam, E. C.-C. Cheng, *Top. Curr. Chem.* **2007**, *281*, 269–309; b) V. W.-W. Yam, E. C.-C. Cheng, *Chem. Soc. Rev.* **2008**, *37*, 1806–1813.
- [7] V. W.-W. Yam, S. W.-K. Choi, T.-F. Lai, W.-K. Lee, *J. Chem. Soc. Dalton Trans.* **1993**, 1001–1002.
- [8] a) V. W.-W. Yam, K. M.-C. Wong, L.-L. Hung, N. Zhu, *Angew. Chem.* **2005**, *117*, 3167–3170; *Angew. Chem. Int. Ed.* **2005**, *44*, 3107–3110; b) K. M.-C. Wong, X. Zhu, L.-L. Hung, N. Zhu, V. W.-W. Yam, H.-S. Kwok, *Chem. Commun.* **2005**, 2906–2908; c) K. M.-C. Wong, L.-L. Hung, W. H. Lam, N. Zhu, V. W.-W. Yam, *J. Am. Chem. Soc.* **2007**, *129*, 4350–4365.
- [9] a) V. K.-M. Au, K. M.-C. Wong, N. Zhu, V. W.-W. Yam, *J. Am. Chem. Soc.* **2009**, *131*, 9076–9085; b) J. J. Yan, A. L.-F. Chow, C.-H. Leung, R. W.-Y. Sun, D.-L. Ma, C.-M. Che, *Chem. Commun.* **2010**, *46*, 3893–3895.
- [10] M. A. Mansour, R. J. Lachicotte, H. J. Gysling, R. Eisenberg, *Inorg. Chem.* **1998**, *37*, 4625–4632.
- [11] a) M. A. Ivanov, M. V. Puzyk, *Russ. J. Gen. Chem.* **2001**, *71*, 1660–1661; b) M. A. Ivanov, M. V. Puzyk, K. P. Balashev, *Opt. Spectrosc.* **2006**, *100*, 382–385.

- [12] E. C. Constable, T. A. Leese, *J. Organomet. Chem.* **1989**, 363, 419–424.
- [13] N. Miyaoura, A. Suzuki, *Chem. Rev.* **1995**, 95, 2457–2483.
- [14] a) D. Fan, C. T. Yang, J. D. Ranford, P. F. Lee, J. J. Vittal, *Dalton Trans.* **2003**, 2680–2685; b) D. Fan, C. T. Yang, J. D. Ranford, J. J. Vittal, P. F. Lee, *Dalton Trans.* **2003**, 3376–3381; c) D. Fan, E. Meléndez, J. D. Ranford, P. F. Lee, J. J. Vittal, *J. Organomet. Chem.* **2004**, 689, 2969–2974.
- [15] R. V. Parish, J. P. Wright, R. G. Pritchard, *J. Organomet. Chem.* **2000**, 596, 165–176.
- [16] a) W. Henderson, B. K. Nicholson, S. J. Faville, D. Fan, J. D. Ranford, *J. Organomet. Chem.* **2001**, 631, 41–46; b) W. Henderson, B. K. Nicholson, A. L. Wilkins, *J. Organomet. Chem.* **2005**, 690, 4971–4977; c) K. J. Kilpin, W. Henderson, B. K. Nicholson, *Polyhedron* **2007**, 26, 204–213; d) K. J. Kilpin, W. Henderson, B. K. Nicholson, *Polyhedron* **2007**, 26, 434–447.
- [17] K. Kubo, A. Nakao, Y. Ishii, R. Kato, G. Matsubayashi, *Synth. Met.* **2005**, 153, 425–428.
- [18] J. Brooks, Y. Babayan, S. Lamansky, P. I. Djurovich, I. Tsyba, R. Bau, M. E. Thompson, *Inorg. Chem.* **2002**, 41, 3055–3066.
- [19] a) K. Ichimura, T. Kobayashi, K. A. King, R. J. Watts, *J. Phys. Chem.* **1987**, 91, 6104–6106; b) X. Y. Wang, R. N. Prabhu, R. H. Schmehl, M. Weck, *Macromolecules* **2006**, 39, 3140–3146.
- [20] P. O'Neill, S. Steenken, D. Schulte-Frohlinde, *J. Phys. Chem.* **1975**, 79, 2773–2779.
- [21] T. A. Gadosy, D. Shukla, L. J. Johnston, *J. Phys. Chem. A* **1999**, 103, 8834–8839.
- [22] S. Komamine, M. Fujitsuka, O. Ito, *Phys. Chem. Chem. Phys.* **1999**, 1, 4745–4749.
- [23] B. Guizzardi, M. Mella, M. Fagnoni, M. Freccero, A. Albini, *J. Org. Chem.* **2001**, 66, 6353–6363.
- [24] T. Nishimura, K. Maeda, S. Ohsawa, E. Yashima, *Chem. Eur. J.* **2005**, 11, 1181–1190.
- [25] a) J. N. Demas, G. A. Crosby, *J. Phys. Chem.* **1971**, 75, 991–1024; b) J. van Houten, R. Watts, *J. Am. Chem. Soc.* **1976**, 98, 4853–4858.
- [26] a) C. M. Che, K. Y. Wong, F. C. Anson, *J. Electroanal. Chem. Interfacial Electrochem.* **1987**, 226, 211–226; b) N. G. Connelly, W. E. Geiger, *Chem. Rev.* **1996**, 96, 877–910.
- [27] D. Gewith, DENZO: *The HKL Manuals—A description of programs DENZO XDISPLAYF and SCALEPACK*, written with the cooperation of the program authors Z. Otwinowski and W. Minor, Yale University, New Haven, **1995**.
- [28] G. M. Sheldrick, SHELXL97, *Program for the Refinement of Crystal Structures*, University of Göttingen, Göttingen, Germany, **1997**.

Received: July 12, 2010
Published online: October 22, 2010